UH-15-38, a potential antiviral drug: Analytical methodology and metabolic profile

A thesis submitted by

Chunhui Li

in partial fulfillment of the requirements for the degree of

Master of Science

in

Pharmacology and Drug Development

Tufts University

Graduate School of Biomedical Sciences

August 2022

Advisors: James D. Baleja, Ph.D, David J. Greenblatt, M.D.

Abstract

An analytical methodology was developed for the quantitation of low concentrations of the antiviral compound UH-15-38 in animal or human plasma. The method utilizes liquid chromatography coupled with mass spectrometry, and has such high sensitivity that it can be applied to in vivo pharmacokinetic studies. The cytochrome P450-mediated Phase I in vitro metabolism of UH-15-38 was studied using a validated human liver microsomal model, together with selective chemical inhibition. With the use of High-Performance Liquid Chromatography linked with Mass Spectrometry (HPLC-MS) four principal metabolites were identified. These were formed by monohydroxylation (M18 and M29), demethylation (M19), and cleavage (M15). Using specific CYP enzyme target inhibitors, it was demonstrated that CYP3A4/5 is the most crucial enzyme in the metabolism of UH-15-38. The finding suggests that inhibitors or inducers of CYP3A might modify the metabolic pathway and pharmacologic effects of UH-15-38 in clinical usage.

Acknowledgments

Throughout the writing of this thesis, I have received a great deal of support and assistance.

First and foremost, I would like to express my sincere gratitude to my supervisor, Dr. David. J. Greenblatt and Dr. James Baleja for their wisdom both in scientific experiments, study and normal life. It does help a lot, especially for an international student like me to feel easy to be infused in American life.

I would like to express my deepest gratitude to Mr. Christopher Singleton. Without his help and advice in metabolism identification and LC-MS method development, this thesis could not have been finished.

I am deeply indebted to the contribution of Dr. Alexei Degterev of compound UH-15-38 that provided the basis of these studies.

I am also thankful for Dr. Md Amin Hossain and Mr. Qingchen Zhang. Their guidance and advice with experimental details helped me greatly

In the end, I want to express my sincere gratitude to my parents and girlfriend. It's their encouragement and patience that supports me overcome 12 hours difference. Even though the mountains and rivers are different, the sky and the moon are still similar.

Table of Contents

List of Tables

List of Figures

List of Abbreviations

AECs: Alveolar Epithelial Cells
AO: Aldehyde oxidase
COVID-19: Coronavirus disease 2019
CYP: Cytochrome P450
DAI: DNA-dependent activator of interferon regulatory factors
DDI: Drug-Drug Interaction
ESI: electrospray ionization
HLM: Human liver microsome
IAVs: Influenza A Viruses
LC-MS: liquid chromatography coupled with mass spectrometry
MLKL: pseudo kinase mixed lineage kinase domain-like
MRM: Multiple reaction monitoring
PBS: Phosphate-buffered saline
RIPK3: receptor-interacting protein kinase 3
UDP: Uridine diphosphate
UGT: UDP-glucuronosyltransferase

Chapter 1: Introduction

As one of the most critical worldwide human health pathogens before the outbreak of the coronavirus disease (COVID-19) pandemic, the seasonal Influenza A Viruses (IAVs) caused an annual average of 12,000-52,000 deaths per year from 2010 to 2020 in the United States. [1]

As one type of lytic virus, the primary infection site of IAVs is the epithelial cells (AECs). The inflammatory responses and degradation of AECs are the main reason for the high morbidity and mortality of IAVs.[2]

Based on previous studies, the receptor-interacting protein kinase 3 (RIPK3) plays a critical role in the multiple-functional cell death pathway. Being located on chromosome 14 in humans, the main function of RIPK3 can be divided into two different cell death directions: Necroptosis and Apoptosis. As shown in Figure 1[3], after the action of DNA-dependent activation of interferon regulatory factors (DAI) following the infection by IAV, the downstream kinase RIPK3 can in turn phosphorylate its target: mixed lineage kinase domain-like pseudokinase (MLKL). With the accumulation of activated MLKL in the ACEs' plasma membrane, cell swelling and lysis will be induced, which is the main cause of AEC degradation. On the other hand, as one of the most important immune mechanisms in the human body, apoptosis caused by the activation of Caspase 8, which also is regulated by RIPK3, cannot be blocked by inhibition of RIPK3.[3]

Based on this, compounds that can specifically inhibit the blockade of RIPK3 phosphorylation of MLKL might play a very important part in IAV treatment.

In previous in vitro experiments[4], compounds in this UH-15 family illustrate this function. The UH-15 family reverses the blockage of separation of inflammatory symptoms and AECs' damage caused by IAVs without interrupting normal immune functions. In addition, the UH-15 family also blocks receptor-interacting protein kinase 2 (RIPK2), which accounts for other inflammatory diseases, including inflammatory bowel disease. [5]

These properties suggest the possibility of clinical benefits for UH-15 compounds in IAV patients. Nevertheless, one major challenge of translating knowledge gained from in-vitro models to clinical trials and treatment applications is drug safety. Experimental models can suggest the pathway to clinical research but are not directly indicative of therapeutic and adverse drug effects in humans.

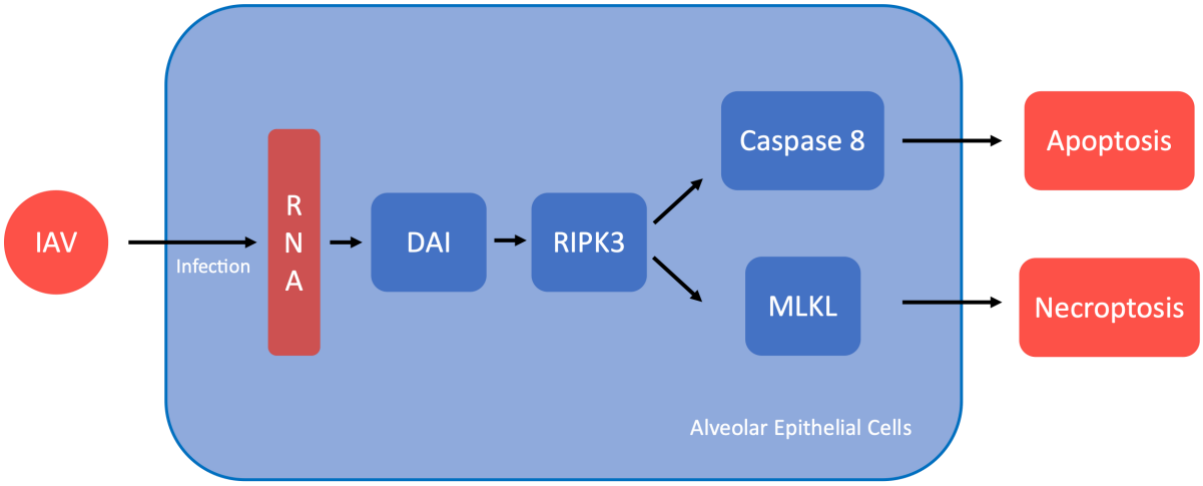

Figure 1.1: Pathway of RIPK3 involvement in IAV

The properties that can be most directly tested in vitro involve drug metabolism and disposition, elimination, and toxicity. Most drug metabolism happens in liver cells (hepatocytes), containing Cytochrome P450 (CYP) metabolic enzymes and non-CYP enzymes, including UDP-glucuronosyltransferases (UGT) and aldehyde oxidases (AO).

During the hepatic metabolism process, there are two main concerns encountered in drug development and in clinical studies. As an example, consider the inhibition effect produced by coadministration of acetaminophen with dasabuvir[6-8], which may produce organ damage as a consequence of polypharmacy (multiple drug coadministration). There may be drug-drug interactions (DDIs), involving either inhibition (leading to an increase of plasma concentration or increase of concentration of toxic metabolites) or induction. Both can have a significant effect on the drug's metabolism, elimination, and clinical effects.

Metabolite identification in human liver microsome studies is a key approach to these two concerns. Not only can it identify potentially toxic metabolites, but also can estimate potential drug-drug interactions after determining the key CYP or UGT isoform types involved in biotransformation, which can be established by using isoform-selective CYP inhibitors to determine the changes in the rate of metabolite formation.

With the purpose of exploring the pharmacokinetics and metabolism of the UH-15 family, the UH-15-38 is used as an example[9,10]. (Its structure is shown in Figure 2.2). In order to study the in vivo pharmacokinetics of UH-15-38, a method was developed to measure concentrations in both animal and human plasma. After that, the metabolites of UH-15-38 were identified using high performance liquid chromatography coupled with mass spectrometry (HPLC-MS), with the background knowledge that CYP3A4 is the most important CYP isoform that metabolizes more than 50% of clinical substrate drugs.[11] After filtering the high-intensity peaks, five CYP isoform enzymes were tested

for relative contribution to in vitro metabolism of UH-15-38 using selected CYP inhibitors. The relationship between specific isoforms and their corresponding inhibitors

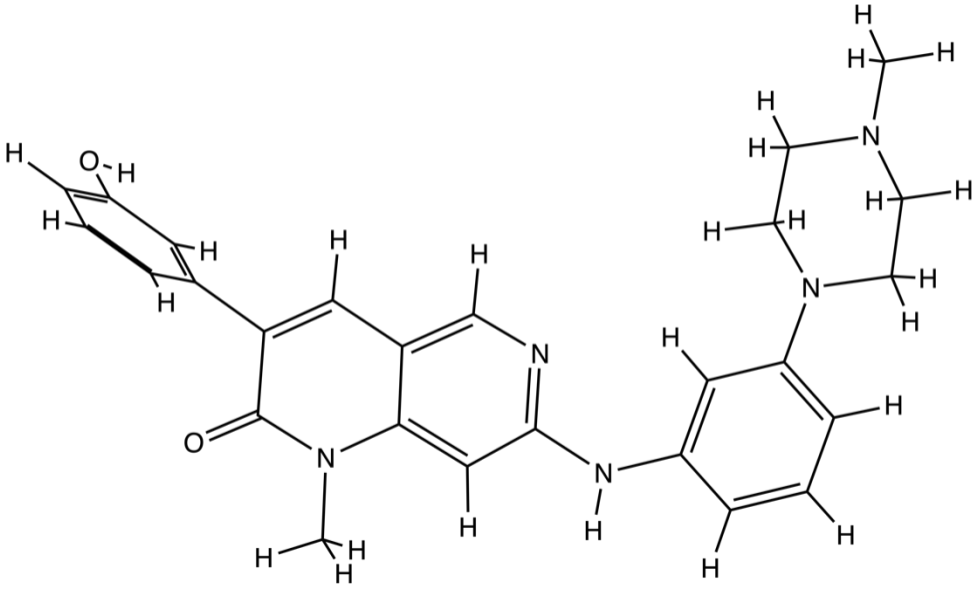

Figure 1.2: Structure of UH-15-38

is shown in Table 1.1.

Fluvoxamine can specifically inhibit the CYP enzyme isoforms identified as CYP1A2 and CYP2C19, with an incubation concentration of 1μM. Ketoconazole specifically inhibits the CYP enzyme isoforms CYP3A4/5, with an incubation concentration of 1μM. Sulfaphenazole inhibits CYP2C9 at a concentration of 5μM, whereas quinidine inhibits CYP2D6 at 5μM. All of these inhibitors have been extensively used in previous studies[12]

Table 1.1: Relationship between enzyme isoform types and their inhibitors' concentration

Inhibitor Name	**CYP Enzyme Isoform Inhibition target**	**Concentration Of Inhibitors**
Fluvoxamine	CYP1A2+CYP2C19	1μM
Ketoconazole	CYP3A4/5	1μM
Sulfaphenazole	CYP2C9	5μM
Quinidine	CYP2D6	5μM

Chapter 2. Materials and Method

2.1 Materials

UH-15-38 was kindly provided by our colleague, Dr. Alexei Degterev. UH-15-38 stock solution was prepared in MS grade methanol (1g/L). These stock solutions were kept at -20℃ and further diluted with methanol for experimental use.

NADPH regeneration systems and buffers for in vitro assays using subcellular fractions were purchased from SEISUI (Kansas City, KS, USA)

The pooled HLM sample was prepared by combining an equal amount of microsomal protein from 22 individual donors, having an age range of 5–74 years.[13] The method for the preparation of HLMs was described previously.[14,15] Briefly, human liver tissue was homogenized three times (w/v) in homogenization buffer (250 mM sucrose and 66.7 mM KH_2PO_4–Na_2HPO_4 at pH = 7.4), then differentially centrifuged at 900 g for 10 min, 13500 g for 10 min, and 105000 g for 30 min. The final sediment was collected and suspended in homogenizing buffer and again centrifuged at 105 000 g, and resuspended in 50 mM KH_2PO_4 buffer (pH = 7.4). The microsomes are stored at −80°C until use. The protein concentration was determined by the bicinchoninic acid assay.[6]

2.2 Laboratory methods

2.2.1 Analysis of Plasma Concentrations

The stock solution of UH-15-38 was diluted to a series of concentrations of calibration standards (0, 0.1 ug/ml, 0.25 ug/ml, 0.5 ug/ml, 1 ug/ml, 2.5 ug/ml), and the

diluted solution was then evaporated to dryness. One group of standards was redissolved in 100 uL PBS, and the other redissolved with the same volume of plasma. Samples were vortexed mixed for 10s. After that, the protein was precipitated by adding 200 uL acetonitrile+0.1% formic acid. After vortexing for 2 minutes, the 96-well plate was centrifuged at 10,000 rpm at 4 C for 10 minutes. In the end, 200 μL of clear supernatant solution was transferred onto a new plate. After evaporating the solvent to dryness, all samples were redissolved with 100 μL mobile phase and vortexed for 1 minute. Samples (10 ul) were injected onto a Waters Acquity HSS column, (2.1×75mm, 1.7um).

2.2.2 Microsomal incubation procedures for metabolite identification and inhibition studies.

The stock solvent was evaporated to dryness after adding specified volumes of the stock solution of UH-15-38, depending on the experiment, to incubation tubes.

The microsomes were pre-diluted with potassium phosphate buffer (KH_2PO_4+K_2HPO_4) (pH=7.4)

In addition to the substrate, the total 250 μl incubation mixture contains 0.25 mg/ml of microsomes and cofactors (NADPH Regenerating System purchased from XenoTech)[16]. A solution of 20 mM potassium phosphate buffer (KH_2PO_4+K_2HPO_4) was used to maintain a physiologic pH of 7.35–7.40. The reaction was initiated by the addition of cofactors and stopped by the addition of another 100 μl ACN. Incubation tubes were kept at 37°C. After the reaction was stopped, samples were then centrifuged at

22 000 g for 10 min to separate the protein, and the supernatant was collected and used for the assay. The incubation time for UH-15-38 was 30 minutes.[17]

The incubation results were analyzed by using a Sciex LC-Q-Trap MS with MRM detection. Sciex Analyst software was used for data acquisition and analysis. LC conditions and MS conditions are provided in Table 2.

Metabolite identification was processed using Sciex MetabolitePilot™ Software 2.0.

2.2.3 Microsomal incubation procedures for Metabolic profiling

The main steps are the same as the previous section, '2.2.2'. The main difference is the addition of the required amount of inhibitors before evaporation of the UH-15-38 diluted solution, whose concentration was 50 μM.

2.2.4 LC-MS Analysis of UH-15-38 Metabolites

Sample analysis was done by high-performance liquid chromatography-mass spectrometry linked with electrospray ionization (HPLC-EMS) on Sciex ZenoTOF 7600 linked with Sciex Robust Clinical HPLC. Incubation samples were placed in an autosampler maintained at 5 °C. Samples (10 ul) were injected onto an ACQUITY UPLC HSS T3 column (1.8 μm, 2.1×150 mm). The components were separated using an Acetonitrile–Water gradient system (Table 2.2.3).

2.2.5 LC-MS/MS Analysis of UH-15-38 for Cytochrome P450 Studies

Samples were analyzed by LC-MS/MS on a SCIEX 5500 QTrap mass spectrometer (Sciex, Redwood City, CA, USA). Incubation samples were injected onto an ACQUITY UPLC HSS T3 column (1.8 um, 2.1×150 mm Column) and separated using a methanol-water gradient system (Table 2.24). The ammonium adducts of UH-15-38 (mass transition 422.1) were analyzed by mass spectrometry using electrospray ionization (ESI) in positive ion mode. The elution method is the same as shown in Table 2.2.5.1

Table 2.1: LC-MS Gradient Conditions for Elution of UH-15-38 and its metabolites

Time(min)	**10mM Ammonium Formate Water Buffer (%)**	**Acetonitrile+0.1% Formic Acid (%)**	**Flow Rate (ml/min)**
0	95	5	0.475
1.5	95	5	0.475
5	75	25	0.475
6.8	75	25	0.475
7	5	95	0.475
10	5	95	0.475

2.3 Contribution of Experiment

The human liver microsomes were kindly prepared by Ms. Suxiang Duan (Part of Section 2.1). The development of HPLC-MS methods for metabolite identification and was done by Mr. Christopher Singleton and me (Section 2.2.2 and Section 2.2.4). All other work was done by me solely.

Chapter 3: Results

3.1 Assay method of UH-15-38 in plasma

Figure 3.1 shows calibration curves for detector response intensity (Y-axis) versus amount of UH-15-38 injected (X-axis) after precipitation from PBS or plasma. The slope of the PBS line is greater (higher) than the slope from plasma, which indicates essentially complete recovery from plasma.

3.2 Metabolite identification

The structure of UH-15-38 is shown in Figure 3.2.1. Figure 3.2.2 illustrates the full mass scan of incubated UH-15-38 in a different LC-MS. After 30 minutes of incubation, four high-intensity metabolites were found. Figure 3.2.3 shows each metabolite peak in the full scan of UH-15-38. The structure and name are generated by Software.

The information on these four metabolites is shown in Table 3.1

3.3 Relationship between metabolism rate and substrate concentration

In addition, the relationship between metabolic rate and substrate concentration was tested. All metabolite peak intensities linearly increased with the increase of the concentration of substrate (Figure 3.3.1). However, there is a large variability between replicate samples shown in all graphs at the highest (50 μM) concentration point, which might be caused by exceeding the maximum detection limit of MS.

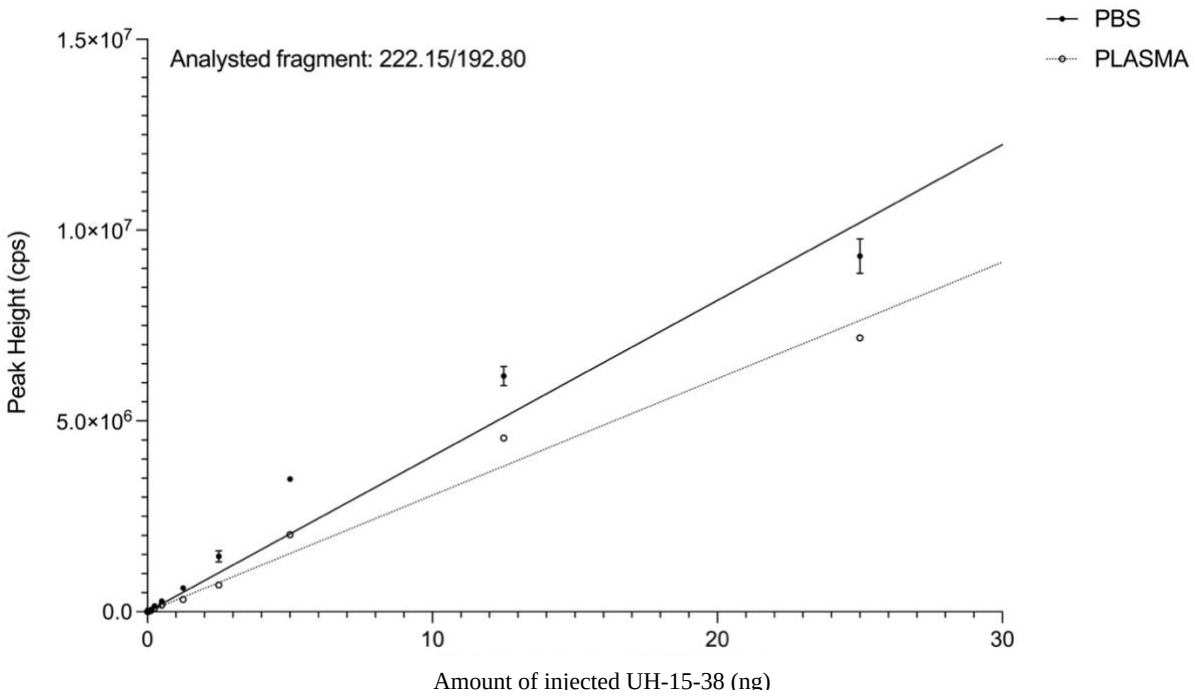

Figure 3.1: Relationship between detector response (Y-axis, cps) versus Quantity of analyte injected (X-axis, ng)

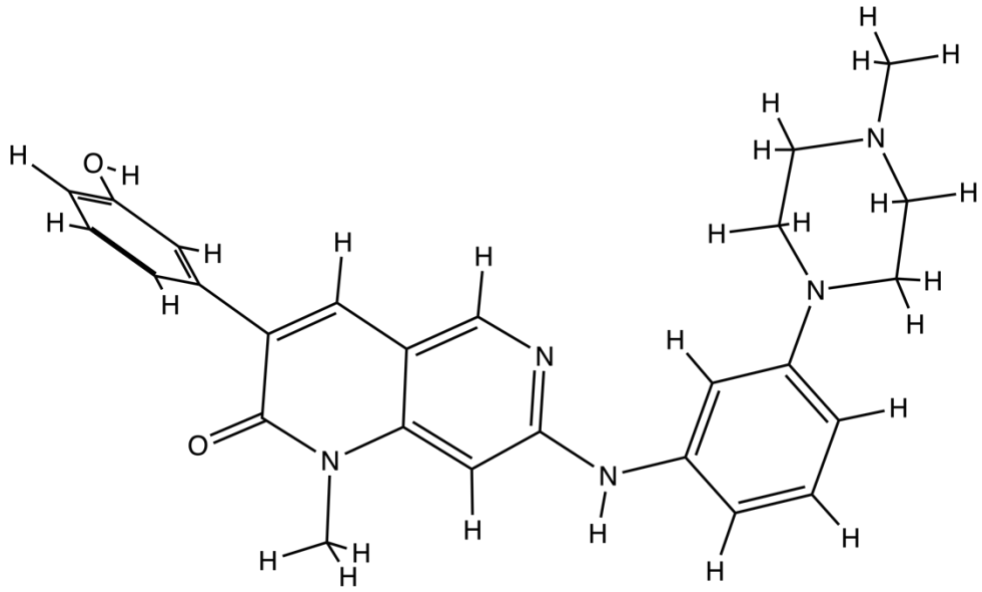

Figure 3.2: The structure of UH-15-38

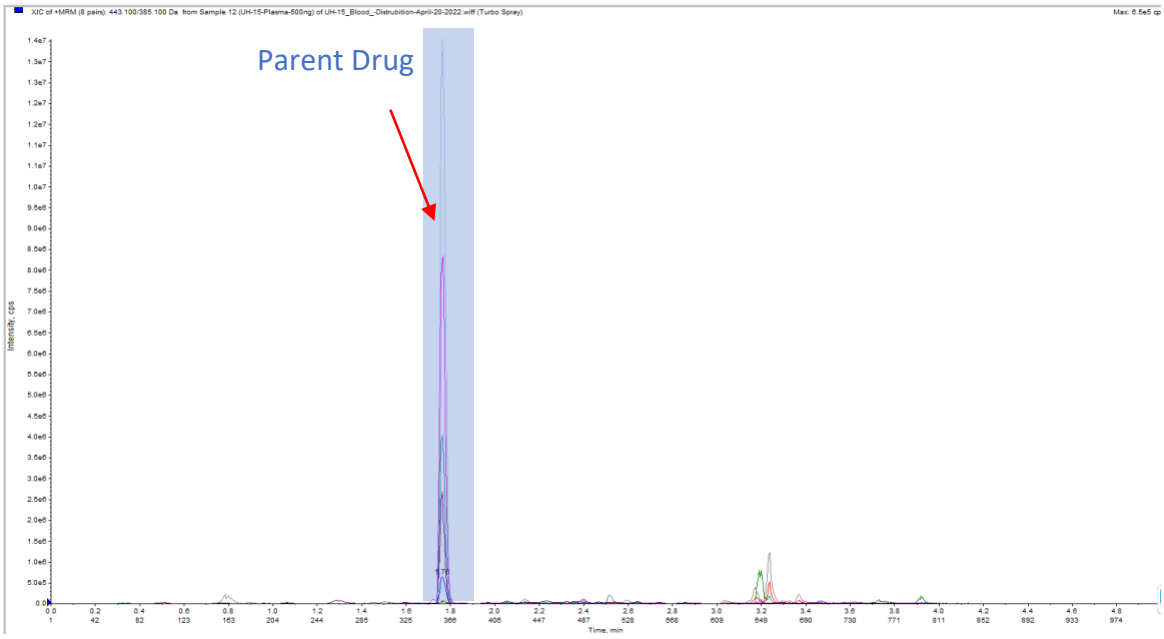

Figure 3.3: Full scan of UH-15-38 incubation Retention time (x-axis) vs metabolite intensity (y-axis)
Analysis was processed using a Waters Acquity HSS column, (2.1X 75mm, 1.7um). Red arrow and blue highlight show the location of the Parent Drug UH-15-38 (RT=1.79)

Table 3.1: UH-15-38 and Metabolite information
m/z is mass divided by charge number, detected by Mass-spectrometry. Based on the molecular weight, the possible structure and metabolic pathway are estimated by MetabolitePilot™ Software 2.0.

Metabolite ID	Metabolism type	Formula	Neutral Mass	m/z	Retention Time (min)
UH-15-38	Parent Drug	$C_{26}H_{27}N_5O_2$	441.50	442.50	4.11
M15	Cleavage	$C_{24}H_{25}N_5O_2$	415.20	416.21	4.03
M18	Hydroxylation	$C_{26}H_{28}N_5O_3$	457.21	457.21	4.19
M19	Demethylation	$C_{25}H_{25}N_5O_2$	427.20	427.20	4.08
M29	Hydroxylation	$C_{26}H_{28}N_5O_3$	457.21	457.21	3.85

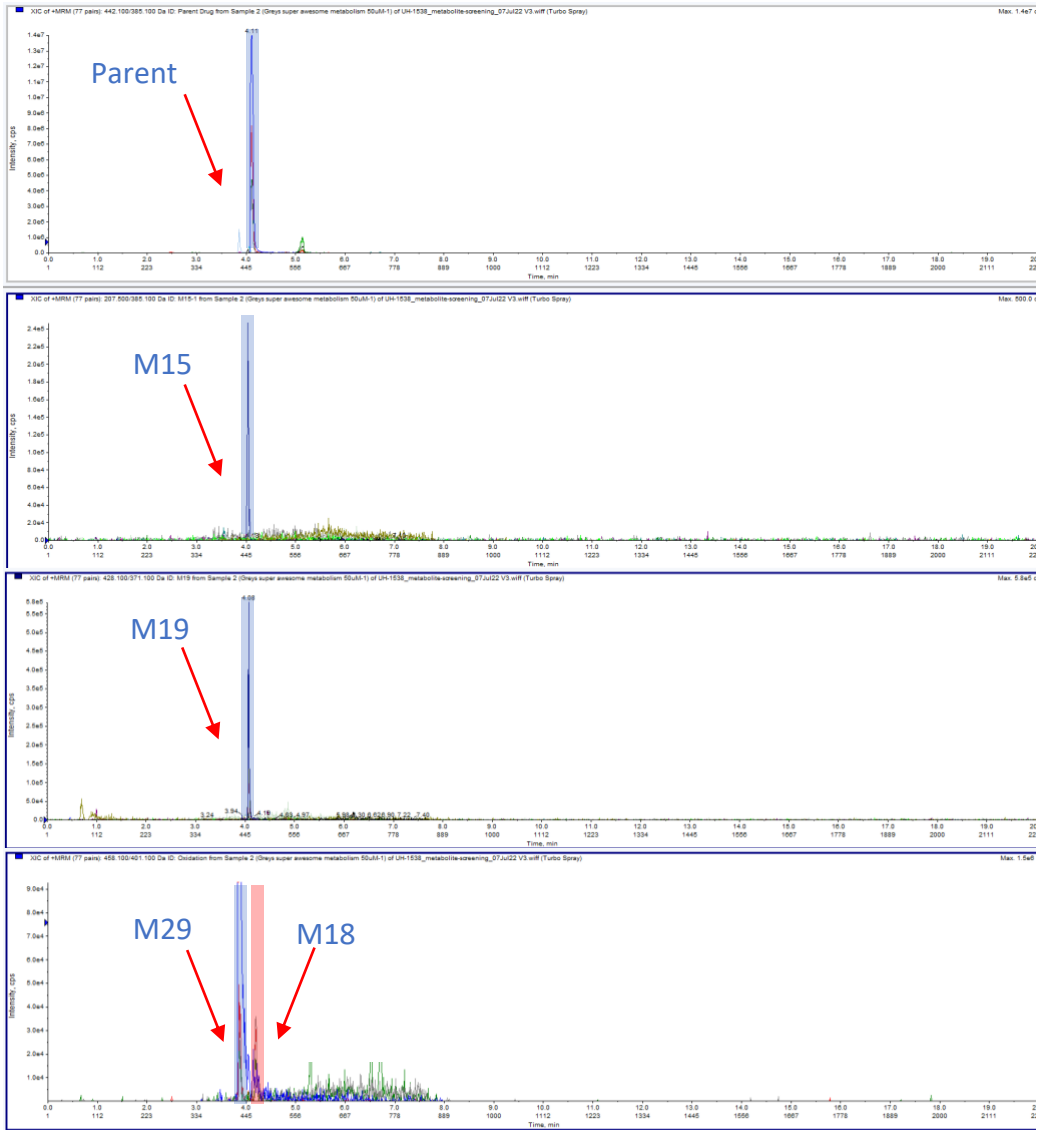

Figure 3.4: Retention time and intensity comparison between Parent drug peak and peaks corresponding to the metabolites.

UH-15-38, M19, M15, and M29 peaks are highlighted by light blue in each panel, and M18 peaks are highlighted in light Red in the third panel. (RT=4.11, 4.03, 4.19, 4.08, 3.85 minutes)

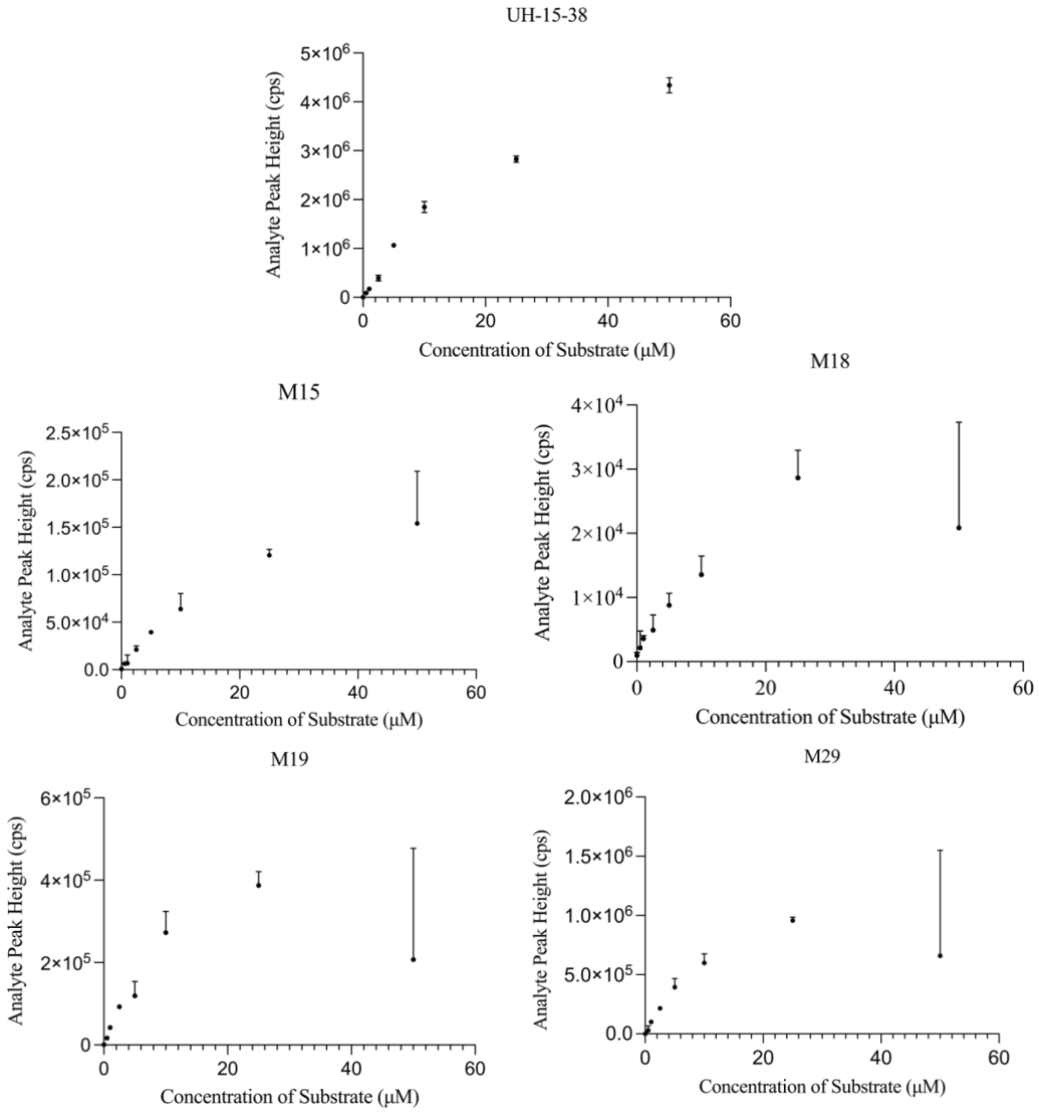

Figure 3.5: Linearity of UH-15-38 metabolism with respect to substrate concentration

The Y axis is the analyte peak height determined from MS analyst (cps), X axis is the concentration of UH-15-38 (μM). The error bar is the standard error.

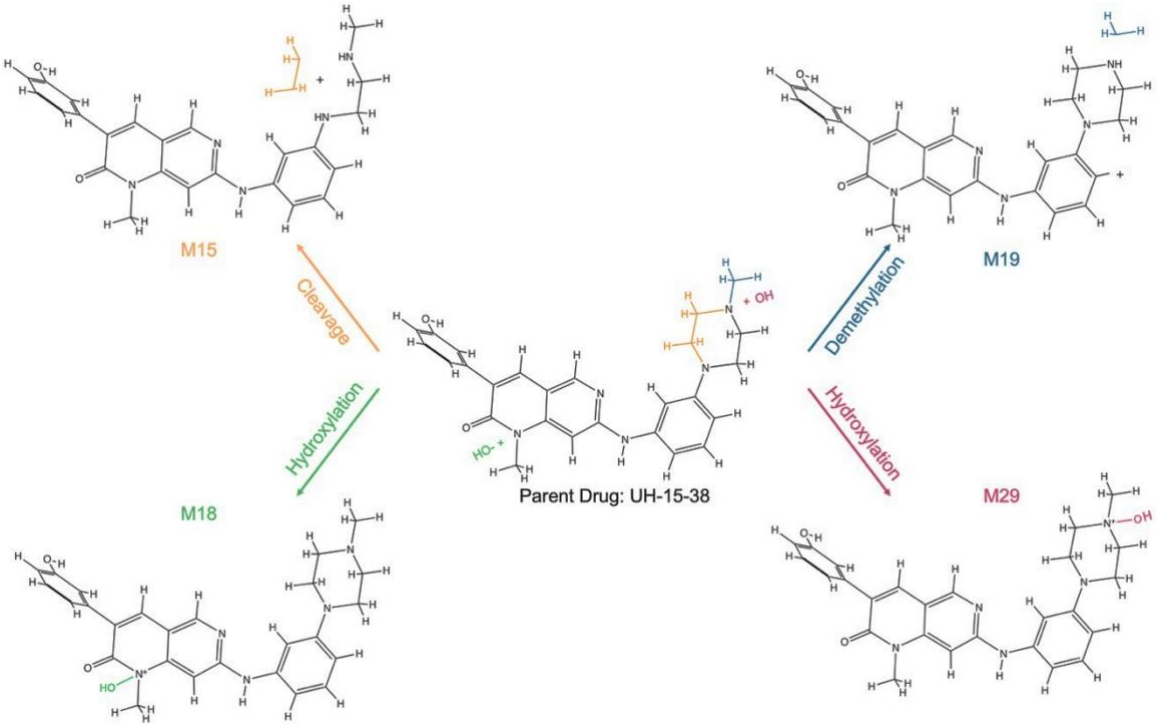

Figure 3.6: Four Potential metabolic reactions of UH-15-38.
Colored parts are the functional groups that have been modified by metabolism

3.4 Cytochrome P450 Metabolism of UH-15-38 Using Chemical Inhibitors

Percent inhibition of UH-15-38's metabolism was calculated by the comparison of metabolite production in samples containing chemical inhibitors to respective blank control samples incubated without inhibitors. The relationship between chemical inhibitors to their specific CYP enzyme isoforms is shown in Table 2.2.3

3.4.1 Inhibition of metabolite formation by specific chemical inhibitors, grouped by their target CYP Isoform

The reduction of peak intensity is reflected by the fraction of the peak height with the addition of inhibitor divided by the control with no inhibitor. A fraction close to 1.0 indicates minimal inhibition, while values close to zero indicate a high degree of inhibition.

The inhibition of UH-15-38 metabolism by direct-acting inhibitors was observed in incubations with Ketoconazole[18] (CYP3A4/5), but not with the other inhibitors. (Figure 3.4.1)

Because the inhibition was only seen with ketoconazole, which is a specific CYP3A4/5 inhibitor, the finding indicates that these metabolites are mainly formed by CYP3A4/5

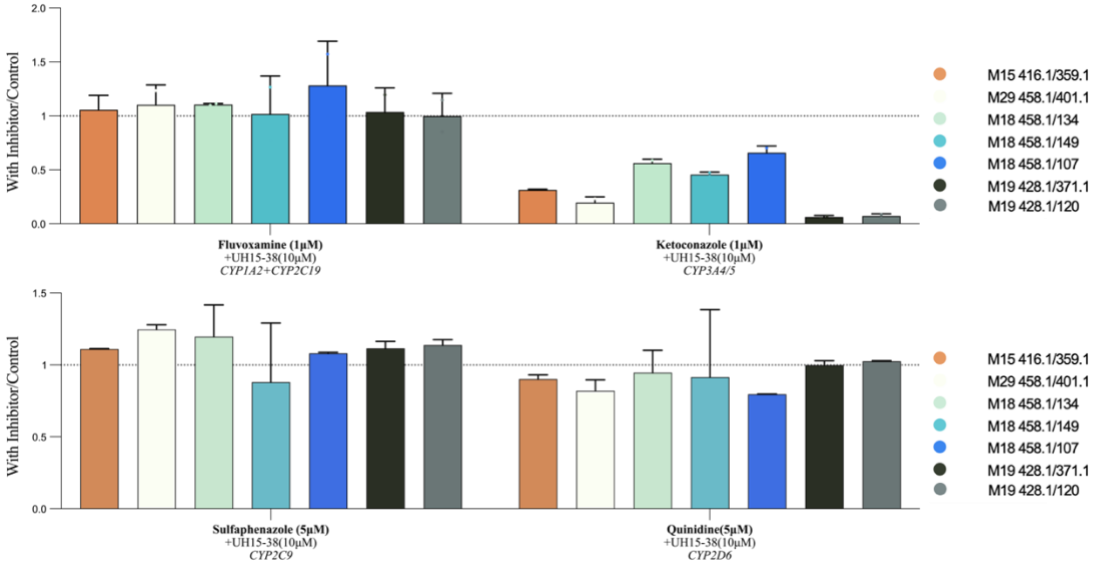

Figure 3.7: Inhibition of metabolite formation by specific chemical inhibitors of metabolite intensity, grouped by their target CYP Isoform
Bars indicate formation of specific metabolites with co-addition of inhibitors, expressed as a fraction of the control value with no inhibitor

3.5 Contribution of Experiment

All figures in this part were done by me solely. Mr. Singleton kindly assisted with HPLC-MS method development and Metabolite Identification procedures (Section 3.2). Other work was done by me solely.

Chapter 4: Discussion

As IAV is a critical worldwide human health pathogen, new and more effective treatments are needed. The present studies used HPLC-MS methods to support pharmacokinetic and metabolic studies needed for the development of UH-15-38 in animals and eventually in humans. A method to analyze UH-15-38 concentrations in plasma was developed for use in basic and clinical pharmacokinetic work on this drug to determine properties such as volume of distribution, half-life (t1/2), and clearance.

The pathway of metabolic clearance of UH-15-38 was also investigated. In order to validate the probable metabolites formed by the CYP enzymes, an HLM metabolism model and HPLC-MS analysis methods have been established, allowing the study of drug metabolism in vitro. After being incubated with the drug in HLM, four metabolites have been found, which are formed by hydroxylation, demethylation, and cleavage.

To determine which CYP isoforms participated in UH-15-38's metabolism, we used four CYP isoform targeted chemical inhibitors. The formation of metabolites is extensively inhibited by the CYP3A4/5 specific antagonist ketoconazole. Only a very limited inhibition effect was observed with other specific inhibitors, indicating that CYP3A4/5 is the main enzyme controlling the formation of UH-15-38 metabolites.

The coadministration of CYP3A4/5 inhibitors with UH-15-38 in clinical use could be an approach to pharmacokinetic boosting, as is now commonly done in the treatment of HIV and hepatitis using ritonavir as the boosting agent.

UGT-mediated metabolism of UH-15-38 is a potentially important pathway of metabolism which remains to be investigated, since an aromatic hydroxy group is found on the benzene ring in UH-15-38. This is a potential site for Phase II conjugation to glucuronic acid. Chemical inhibition of this metabolic step would be another possible approach to boosting, allowing a delay in the clearance of UH-15-38 and prolongation of its effect.

Chapter 5: Bibliography

1. Roberts Jr NJ, Krilov LR. The Continued Threat of Influenza A Viruses. MDPI; 2022. p. 883.
2. Brazee PL, Morales-Nebreda L, Magnani ND, et al. Linear ubiquitin assembly complex regulates lung epithelial–driven responses during influenza infection. *The Journal of clinical investigation*. 2020;130(3):1301-1314.
3. Najjar M, Saleh D, Zelic M, et al. RIPK1 and RIPK3 kinases promote cell-death-independent inflammation by Toll-like receptor 4. *Immunity*. 2016;45(1):46-59.
4. Shubina M. *Influenza A Virus Induced Programmed Cell Death*. Temple University; 2020.
5. P Li A. In vitro human hepatocyte-based experimental systems for the evaluation of human drug metabolism, drug-drug interactions, and drug toxicity in drug development. *Current topics in medicinal chemistry*. 2014;14(11):1325-1338.
6. Zhang Q, Duan SX, Harmatz JS, Wei Z, Singleton CA, Greenblatt DJ. Mechanism of dasabuvir inhibition of acetaminophen glucuronidation. *Journal of Pharmacy and Pharmacology*. 2022;74(1):131-138.
7. Ameer B, Greenblatt DJ. Acetaminophen. *Annals of internal Medicine*. 1977;87(2):202-209.
8. Yoon E, Babar A, Choudhary M, Kutner M, Pyrsopoulos N. Acetaminophen-induced hepatotoxicity: a comprehensive update. *Journal of clinical and translational hepatology*. 2016;4(2):131.
9. Von Moltke LL, Greenblatt DJ, Grassi JM, et al. Multiple human cytochromes contribute to biotransformation of dextromethorphan in-vitro: role of CYP2C9, CYP2C19, CYP2D6, and CYP3A. *Journal of pharmacy and pharmacology*. 1998;50(9):997-1004.
10. Giancarlo GM, Venkatakrishnan K, Granda BW, von Moltke LL, Greenblatt DJ. Relative contributions of CYP2C9 and 2C19 to phenytoin 4-hydroxylation in vitro: inhibition by sulfaphenazole, omeprazole, and ticlopidine. *European journal of clinical pharmacology*. 2001;57(1):31-36.
11. Hesse LM, Venkatakrishnan K, von Moltke LL, Shader RI, Greenblatt DJ. CYP3A4 is the major CYP isoform mediating the in vitro hydroxylation and demethylation of flunitrazepam. *Drug metabolism and disposition*. 2001;29(2):133-140.
12. Venkatakrishnan K, von Moltke LL, Greenblatt DJ. Human drug metabolism and the cytochromes P450: application and relevance of in vitro models. *The Journal of Clinical Pharmacology*. 2001;41(11):1149-1179.
13. Alam N, Angeli MG, Greenblatt DJ. Mechanism of in-vitro inhibition of UGT1A1 by paritaprevir. *Journal of Pharmacy and Pharmacology*. 2017;69(12):1794-1801.
14. Chamberlain J, Jagarinec N, Ofner P. Catabolism of C19-steroids by subcellular fractions of mammalian and avian tissues. I. Hydroxylation of ring A-saturated substrates by rat-liver microsomes. *Steroids*. 1965:Suppl 2: 1-12.
15. Von Moltke LL, Manis M, Harmatz JS, Poorman R, Greenblatt DJ. Inhibition of acetaminophen and lorazepam glucuronidation in vitro by probenecid. *Biopharmaceutics & drug disposition*. 1993;14(2):119-130.

16. Luo D, Luesch H. Ahp-cyclodepsipeptide inhibitors of elastase: lyngbyastatin 7 stability, scalable synthesis, and focused library analysis. *ACS medicinal chemistry letters*. 2020;11(4):419-425.
17. Bertelsen KM, Venkatakrishnan K, Von Moltke LL, Obach RS, Greenblatt DJ. Apparent mechanism-based inhibition of human CYP2D6 in vitro by paroxetine: comparison with fluoxetine and quinidine. *Drug Metabolism and Disposition*. 2003;31(3):289-293.
18. Greenblatt DJ, Venkatakrishnan K, Harmatz JS, Parent SJ, von Moltke LL. Sources of variability in ketoconazole inhibition of human cytochrome P450 3A in vitro. *Xenobiotica*. 2010;40(10):713-720.